⌘ *Author's Choice*

THE JOURNAL OF BIOLOGICAL CHEMISTRY VOL. 285, NO. 37, pp. 28683–28690, September 10, 2010


# Base Excision Repair in a Glucocorticoid Response Element

## *EFFECT OF GLUCOCORTICOID RECEPTOR BINDING*[*] [S]

Received for publication, February 11, 2010, and in revised form, June 16, 2010 Published, JBC Papers in Press, July 13, 2010, DOI 10.1074/jbc.M110.113530

**Angela K. Hinz, Yan Wang, and Michael J. Smerdon**[1]

*From Biochemistry and Biophysics, School of Molecular Biosciences, Washington State University, Pullman, Washington 99164-7520*

**DNA repair takes place in the context of chromatin. Previous studies showed that histones impair base excision repair (BER) of modified bases at both the excision and synthesis steps. We examined BER of uracil in a glucocorticoid response element (GRE) complexed with the glucocorticoid receptor DNA binding domain (GR-DBD). Five substrates were designed, each containing a unique C→U substitution within the mouse mammary tumor virus promoter, one located within each GRE half-site and the others located outside the GRE. To examine distinct steps of BER, DNA cleavage by uracil-DNA glycosylase and Ape1 endonuclease was used to assess initiation, dCTP incorporation by DNA polymerase (pol) β was used to measure repair synthesis, and DNA ligase I was used to seal the nick. For uracil sites within the GRE, there was a reduced rate of uracil-DNA glycosylase/Ape1 activity following GR-DBD binding. Cleavage in the right half-site, with higher GR-DBD binding affinity, was reduced ~5-fold, whereas cleavage in the left half-site was reduced ~3.8-fold. Conversely, uracil-directed cleavage outside the GRE was unaffected by GR-DBD binding. Surprisingly, there was no reduction in the rate of pol β synthesis or DNA ligase activity on any of the fragments bound to GR-DBD. Indeed, we observed a small increase (~1.5–2.2-fold) in the rate of pol β synthesis at uracil residues in both the GRE and one site six nucleotides downstream. These results highlight the potential for *both* positive and negative impacts of DNA-transcription factor binding on the rate of BER.**

DNA damage occurs in the cell by an array of genotoxic agents, both endogenous and exogenous. The effect of DNA damage on basic housekeeping functions of the cell depends on the nature of the lesion. Eukaryotic cells remove DNA lesions through two major pathways: nucleotide excision repair and base excision repair (BER).[2] Nucleotide excision repair is responsible for the removal of bulky lesions in DNA, whereas BER removes primarily small, non-helix-distorting lesions (1).

Large bulky adducts between adjoining nucleotides have been shown to physically block access of proteins necessary for cellular maintenance such as replication and transcription (2). Indeed, we have previously shown that binding of transcription factor IIIA to the 5 S rRNA gene decreases the rate of repair of UV radiation-induced cyclobutane pyrimidine dimers located in the internal control region (3). Furthermore, introduction of single cyclobutane pyrimidine dimer lesions at six different sites in the internal control region of 5 S rDNA allowed us to map the binding strength of transcription factor IIIA to its cognate sequence (4, 5). Although overall binding was unaltered, cyclobutane pyrimidine dimer damage at certain sites increased the dissociation rate of transcription factor IIIA by up to 4-fold. Moreover, the higher off rate correlated with an increased repair rate (4, 5), suggesting that the rate of DNA damage recognition is determined, in part, by existing protein·DNA complexes.

Base excision repair is responsible for the repair of DNA lesions that result from modification of the nitrogenous bases. These lesions are caused by a variety of sources, including exogenous agents like alkylating chemicals and endogenous events like replication errors and oxidative damage. In eukaryotic cells, damaged bases are recognized and removed by specialized enzymes, collectively known as DNA glycosylases. Each glycosylase recognizes one or more specific lesions and removes the damaged base (6). Furthermore, the glycosylase serves to protect the abasic site by possessing a higher binding affinity for abasic sites than the original damaged base (7). Subsequent steps in the BER pathway are believed to proceed in a measured and orderly fashion that has been likened to the "passing of a baton" (8, 9). Endonuclease Ape1 is the second enzyme recruited to the damage site, displacing the glycosylase and creating a single strand nick in the DNA 5′ to the damaged base. At this point, BER can proceed down one of two pathways: long patch repair (2–10-nucleotide replacement) or DNA polymerase β (pol β)-dependent short patch repair (one-nucleotide replacement). During short patch repair, pol β displaces Ape1, removes the deoxyribose sugar, and uses the complementary base as a template to insert the correct nucleotide. Finally, DNA ligase I seals the nick (10).

Similar to examples involving bulky adducts, the binding and affinity of regulatory proteins such as transcription factors are sometimes altered when the regulatory element contains oxidative damage (11, 12). In addition, these protein-DNA interactions can block access of repair proteins to DNA lesions. Indeed, we demonstrated that the activity of pol β is completely suppressed when damaged DNA is associated with a nucleosome (13). This is most likely due to the prevention of signifi-

* This work was supported, in whole or in part, by National Institutes of Health Grant ES004106 from the NIEHS.

⌘ *Author's Choice*—Final version full access.

[S] The on-line version of this article (available at http://www.jbc.org) contains supplemental Figs. S1–S4.

[1] To whom correspondence should be addressed. Tel.: 509-335-6853; Fax: 509-335-9688; E-mail: smerdon@wsu.edu.

[2] The abbreviations used are: BER, base excision repair; GRE, glucocorticoid response element; GR-DBD, glucocorticoid receptor DNA binding domain; MMTV, mouse mammary tumor virus; UDG, uracil-DNA glycosylase; pol, DNA polymerase; EMSA, electrophoretic mobility shift assay; PCI, phenol: chloroform:isoamyl alcohol; LH, left half-site; RH, right half-site; FL, full-length.

cant DNA bending by the DNA·histone complex, which is a requirement for pol β function (14). Thus, protein interactions with damaged DNA can affect the recognition and subsequent repair of DNA.

In this study, we examined BER in a DNA·protein complex where the protein binds just one side of the DNA helix. We used the well characterized glucocorticoid receptor and its cognate sequence, the glucocorticoid response element (GRE), to test the activity of BER enzymes UDG, Ape1, pol β, and DNA ligase I on uracil residues located within (or just outside) a GRE. We showed that the impact of the glucocorticoid receptor DNA binding domain (GR-DBD) binding on opposite sides of the DNA helix from uracil yields both negative and positive effects on the UDG/Ape1 and pol β steps, respectively.

## EXPERIMENTAL PROCEDURES

*Oligos*—Oligomers were purchased from Integrated DNA Technologies. Radiolabeling of the 5′-end was achieved by T4 polynucleotide kinase (Fermentas) and [γ-$^{32}$P]ATP (PerkinElmer Life Sciences). Oligos were annealed to their complement and gel-purified. Briefly, bands were excised and eluted from the gel in 0.3 M NaOAc overnight at 37 °C. The supernatant was extracted with phenol:chloroform, ethanol-precipitated, and subjected to further purification on a spin column via the Nucleotide Removal kit (Qiagen). Samples were spotted onto Whatman paper and assayed by scintillation counting, and the specific radioactivity was quantified.

*GR-DBD Protein*—Segment Cys$^{440}$–Gly$^{525}$ of the rat glucocorticoid receptor was overexpressed from plasmid pGR440 (a gift from Dr. Keith Yamamoto, University of California, San Francisco) in *Escherichia coli* and purified using ammonium sulfate saturation prior to separation on CM-Sepharose. Peak fractions containing GR-DBD were further purified on a Superdex 75 column (supplemental Fig. S1). Pure GR-DBD was dialyzed against 10 mM Hepes (pH 7.6), 1 mM DTT, 10% glycerol, 10 μM $ZnCl_2$, and 0.1 mM EDTA and then stored at −80 °C. Only fractions containing homogeneous GR-DBD (*e.g.* fractions 19–24; supplemental Fig. S1) were utilized in these studies.

*EMSA*—Radiolabeled damaged and undamaged DNA substrates at varying concentrations were incubated with 80 pmol of GR-DBD in binding buffer (10 mM Hepes (pH 7.9), 2.5 mM $MgCl_2$, 0.05 mM EDTA, 10% glycerol, 50 mM NaCl, 0.1% Triton X-100, 1 mM DTT, 2.5 ng/μl poly(dI-dC), and 10 μM $ZnCl_2$) for 30 min at 37 °C. Complexes were resolved on 5% polyacrylamide gels, which were dried and exposed to PhosphorImager screens (GE Healthcare). Quantification was performed using ImageQuant software (GE Healthcare).

Concentrations of bound and free DNA were calculated from the intensities of the DNA bands and the total concentrations of DNA. The ratio of [bound] *versus* [bound]/[free] was plotted, and the slope ($m$) was calculated by linear regression. The $K_d$ value was then determined using $K_d = (-1/m)$ (16).

*Methylation Protection*—End-labeled damaged and undamaged substrates (0.5 pmol) were incubated with 3.2 pmol of GR-DBD in 40 μl of binding buffer at 37 °C for 30 min. One microliter of 8% dimethyl sulfate in ethanol was added, and the incubation continued for 2 min. The samples were then loaded onto 10% native polyacrylamide gels to separate bound from free DNA. Both bound and free bands were excised from the gel, cleaved into small pieces, and soaked in 300 μl of 0.3 M NaOAc at room temperature overnight. The DNA was ethanol-precipitated, and the pellet was dissolved in 70 μl of 10% piperidine and incubated at 90 °C for 30 min. The samples were then dried and washed with water three times before loading onto a 7 M urea and 10% polyacrylamide sequencing gel.

*UDG/Ape1 Cleavage Assay*—*E. coli* UDG and human Ape1 were purchased from New England Biolabs, and human UDG was a gift from Dr. Samuel Wilson, NIEHS, National Institutes of Health. Double-stranded DNA substrates, with the top strands 5′-end-labeled with $^{32}$P, were exposed to 1 μM GR-DBD in reaction buffer containing 50 mM Hepes (pH 7.5), 2 mM DTT, 0.2 mM EDTA, 100 μg/ml BSA, 10% glycerol, 5 mM $MgCl_2$, and 4 mM ATP for 30 min at 37 °C prior to adding UDG and Ape1 (0.025 nM final concentration) and continuing the incubation at 37 °C. Reactions without GR-DBD were exposed to reaction buffer only. The concentrations of UDG and Ape1 were optimized so that we could examine linear enzyme activity, which was achieved when 40–50% of the initial input fragments remained intact after the maximum incubation time (20 min) (supplemental Fig. S2A). Reaction rates were calculated using the slope of the line generated by plotting the percentage of full-length product *versus* time in the first 10 min of the reaction. Experiments were repeated at least three times. At the noted time points, aliquots were removed and immediately extracted with phenol:chloroform:isoamyl alcohol (PCI) to terminate the reaction. Samples were then added to formamide loading buffer and separated on a 7 M urea and 10% denaturing polyacrylamide gel. Gels were soaked in 5% acetic acid, 10% methanol, and 0.5% glycerol for 30 min after electrophoresis and dried before exposing to a PhosphorImager screen.

*Polymerase β Repair Synthesis Assay*—Pol β was a gift from Dr. Samuel H. Wilson, NIEHS, National Institutes of Health. Unlabeled substrate was generated by annealing the two oligonucleotides and subsequent treatment with a Qiagen Nucleotide Removal kit. The reaction mixtures contained the same buffer as described above and 16 pM substrate. After cleavage for 1 h with 10 nM UDG and Ape1, 1 μM GR-DBD was added for 15 min at 37 °C. The time course began with addition of 0.05 nM pol β and 1 μl of 2000 μCi/ml [α-$^{32}$P]dCTP (PerkinElmer Life Sciences). At various times, aliquots were removed and PCI-extracted to stop the reaction. Gels were run and treated as described above. The concentration of pol β was optimized so that we could examine linear enzyme activity, which was achieved at 0.05 nM (supplemental Fig. S2B).

*DNA Ligase I Assay*—DNA ligase I was a gift from Dr. Samuel Wilson, NIEHS, National Institutes of Health. Unlabeled annealed substrate was treated with 10 nM UDG, 10 nM Ape1, 0.05 nM pol β, and 1 μl of 2000 μCi/ml [α-$^{32}$P]dCTP. The resulting labeled substrate was purified by PCI extraction and subsequent ethanol precipitation. Using the same buffer as described above, 4 pmol of substrate were exposed to 100 nM DNA ligase I in the presence or absence of GR-DBD. At various times, aliquots were removed and PCI-treated to stop the reaction. Gels were run and treated as described above. Percent

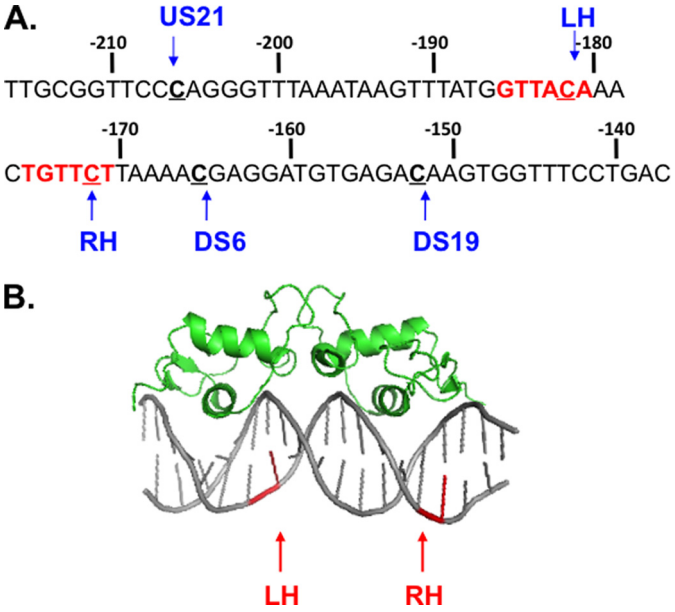


FIGURE 1. **Region of MMTV promoter showing locations of dU incorporation.** *A*, top strand of the MMTV promoter (−216 to −137) containing the GRE. *Red letters* denote the conserved hexamer sequences. The names and locations of the mutated endogenous cytosine residues (*underlined*) are in *blue*. *B*, positioning of LH and RH uracil residues (*red*) in GRE DNA bound to GR-DBD dimer (*green*). (The figure was created using PyMOL, and the structure (Protein Data Bank code 1R4R) is from Luisi *et al.* (15)).

ligase activity was determined as the amount of cleaved product that shifts to full length.

## RESULTS

*Selection of Damaged and Undamaged MMTV Substrates*—The MMTV long terminal repeat promoter is a rich source of regulatory elements and has been used extensively in the characterization of the interaction between the GR and its cognate DNA sequence, the GRE (17, 18). Indeed, there are four GREs within ~200 bases upstream from the transcriptional start site, each consisting of a 15-bp sequence with two conserved hexanucleotide sequences separated by three variable nucleotides (19). The three variable nucleotides serve as a spacer that places both hexamers on the same side of the DNA helix (15), a configuration that facilitates receptor dimerization (20–22). The affinity of the GR is higher for the right half-site, a consensus hexamer with the sequence TGTTCT, than for the left half-site, which can differ in sequence composition.

For these studies, we used an 80-bp region (−216 to −137) of the MMTV promoter that encompasses a single GRE. This distal GRE was identified as the most sensitive to mutation (23), resulting in up to a 20-fold reduction of hormone-dependent transcription when mutated in the right half-site. To examine the effect of a uracil base substitution within the boundaries of the GRE, we generated constructs in which an endogenous cytosine within each half-site (left half-site (LH) and right half-site (RH)) was mutated to a uracil. In addition, endogenous cytosines were mutated to uracil both upstream (US21) and downstream (DS6 and DS19) from the GRE. The numerical designation of the constructs indicates the distance in nucleotides from the GRE (see Fig. 1*A*). Furthermore, using the data of Luisi *et al.* (15), it can be seen that the uracils incorporated in the LH and RH substrates are located on opposite sides of the DNA helix from the GR-DBD binding surface (Fig. 1*B*). These locations have not been identified as regions of interaction with the GR-DBD and are not expected to interfere with GR-DBD binding to the GRE (see below).

*Binding of GR-DBD to dU-damaged Substrate*—We initially determined the DNA binding characteristics of GR-DBD to the high affinity RH substrate. For these studies, the binding constant of GR-DBD to damaged and undamaged constructs was determined by EMSA using increasing amounts of DNA and a constant amount of protein (21). In each experiment, binding of the uracil-damaged construct was compared with that of the undamaged GRE construct (WT). As seen in Fig. 2*A*, the binding constants for undamaged GRE (WT) and RH are 0.82 and 0.85 nM, respectively. Thus, the binding affinity of GR-DBD to the uracil-damaged GRE constructs is equivalent to that of the undamaged constructs.

To ensure that both half-sites of the GRE were bound in subsequent repair experiments, saturating concentrations of GR-DBD were used. A concentration of 1 μM GR-DBD shifted all free DNA into a complex as demonstrated for the US21 construct in Fig. 2*B* (*left panel*). On the other hand, the non-GRE-containing constructs yielded no specific gel shift at this concentration (Fig. 2*B*, *right panel*). In the latter case, the conserved hexamer sites were mutated to CACCTC (left) and CAUCTC (right) to abrogate specific GR-DBD binding while maintaining the uracil in a position similar to that in the RH. (We note that concentrations over 1 μM GR-DBD resulted in a smear of nonspecific binding of the (−) GRE construct (data not shown).) We concluded that each GRE half-site was occupied at 1 μM GR-DBD, and this concentration was used for all subsequent experiments.

Finally, methylation protection assays were performed to evaluate, in detail, the GR-DBD binding characteristics of the uracil-containing constructs. As shown in Fig. 2*C*, the guanine bases within the GRE were protected from methylation by dimethyl sulfate when GR-DBD was present. Specifically, guanines 185 and 175 were protected in both the RH and WT constructs in the top strand. The same was observed for the complementary guanines in the bottom strand opposite cytosines 172 and 181 (data not shown). Together with the EMSA data, these results indicate that the presence of uracil in the GRE of our constructs had little effect on the binding of GR-DBD.

*UDG/Ape1 Cleavage of Damaged Substrates in Presence or Absence of GR-DBD*—The early steps of BER can be reconstituted *in vitro* using commercially available recombinant enzymes. Our initial analysis utilized *E. coli* UDG and human Ape1 (New England Biolabs). Using 5′-end-labeled GRE fragments, we examined the reduction of full-length product following incubation with UDG/Ape1 in the presence or absence of GR-DBD. Interestingly, only uracil residues located within the RH and LH portions of the GRE showed a significantly reduced rate of cleavage. Fig. 3*A* shows representative denaturing gels of the reduction of full-length product over time (*insets*) as well as plots of the fraction of full-length (FL) fragment remaining. From the initial slopes of these data, a "rate of cleavage" (Δpercent FL/Δunit time) was obtained. We note that

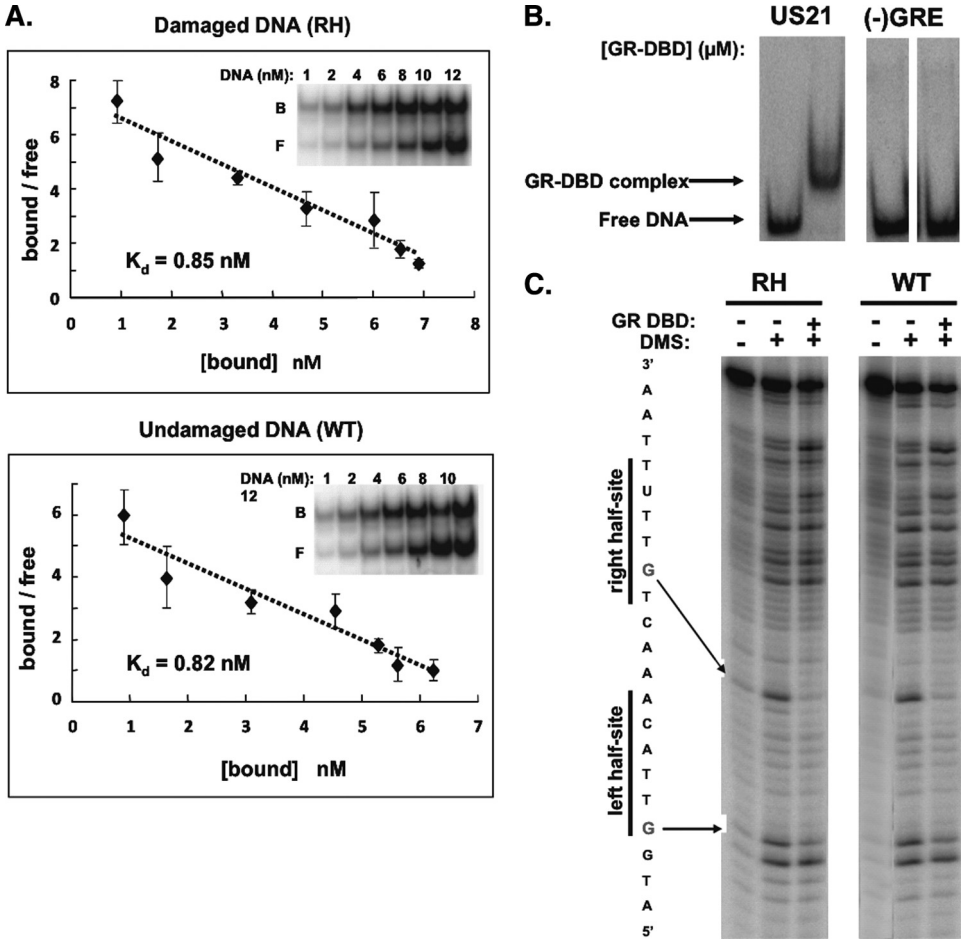


FIGURE 2. **Comparison of GR-DBD binding to dU-damaged and undamaged MMTV DNA.** *A*, determination of apparent $K_d$ values of the GR-DBD·DNA complexes. Panels show EMSA gels (*insets*) and Scatchard analyses (*graphs*) of GR-DBD·damaged DNA complexes (*left panel*) and GR-DBD·undamaged DNA complexes (*right panel*). The ratio of [bound DNA] to [free DNA] was determined from gel scans and plotted *versus* [bound DNA]. $K_d$ values were calculated from the slopes (*m*) of linear regression fits of the data ($K_d = -1/m$). Each data point represents the mean ± 1 S.D. of three independent experiments. *B*, EMSA of MMTV fragments with (US21) and without (*(−)GRE*) a GRE sequence. *C*, methylation protection of MMTV DNA by GR-DBD. The 5′-end of the top strands of dU-damaged (*RH*) and intact (*WT*) DNA were labeled and treated with dimethyl sulfate (*DMS*) in the presence (+) or absence (−) of GR-DBD. DNA was isolated, cleaved with 10% piperidine, and separated on a DNA sequencing gel. *Arrows* denote the positions of G residues in the RH and LH of GRE.

there was an initial drop in cleavage by ~10% at time 0. In addition, cleavage was reduced by ~5-fold for RH and ~3.8-fold for LH in the presence of GR-DBD protein. In contrast, the rate of cleavage of uracil residues in locations just outside of the GRE was only slightly affected by the presence of GR-DBD (Fig. 3*B*).

We repeated these experiments using human UDG in combination with the human Ape1. Not only did we obtain inhibition of human UDG/Ape1 cleavage with GR-DBD binding but the human enzyme showed a more pronounced inhibition (Fig. 3*C*). Indeed, the human UDG/Ape1 reaction was almost completely inhibited in the presence of GR-DBD binding.

In an attempt to determine whether the reduced rate of cleavage was UDG- or Ape1-dependent, we assayed the independent activities of UDG and Ape1 plus or minus GR-DBD. In all experiments, reaction conditions and enzyme concentrations were as described for the UDG/Ape1 assay. To test UDG activity, substrates LH and RH were treated with UDG ± GR-DBD, and aliquots were removed at various time points. After PCI extraction, they were treated with Ape1. To test Ape1 activity, substrates LH and RH were treated with UDG and then PCI-extracted prior to the addition of Ape1 ± GR-DBD (supplemental Fig. S3). Clearly, separation of these activities resulted in reduced efficiency for both UDG and Ape1. Furthermore, the presence of GR-DBD appeared to affect both the UDG and Ape1 steps (although because of the greatly reduced efficiency of these reactions, the data were not analyzed for rate determination).

*Pol β Activity in Presence or Absence of GR-DBD*—Short patch repair synthesis can be promoted *in vitro* by the addition of purified pol β to substrates containing nicked abasic sites. By adding pol β and a radiolabeled cytosine to unlabeled substrates, we monitored the incorporation of cytosine at nicked abasic sites over time in DNA with and without GR-DBD bound. Initially, EMSA was used to show that, as expected, GR-DBD was able to bind nicked abasic DNA similarly to unnicked DNA in the presence of the high concentrations of UDG and Ape1 used in the following assay (supplemental Fig. S4). We then examined pol β-dependent incorporation of radiolabeled cytosine at the nicked abasic sites in the GR-DBD complex. As shown in Fig. 4*A*, pol β incorporation at the abasic site located in the RH portion of the GRE (see Fig. 1*A*) was not inhibited by GR-DBD binding. Indeed, when band intensities from several experiments, normalized to the band intensity at 20 min for naked DNA, were plotted as percentage of incorporation *versus* time, there appeared to be an *enhancement* of pol β incorporation in the presence of GR-DBD (Fig. 4*A*). The initial slopes of these lines, reflecting Δpercent incorporation/Δunit time of pol β incorporation for the various substrates shown in Fig. 1*A*, are given in Fig. 4*B*. Surprisingly, the rates for pol β incorporation show a small, yet statistically significant increase for both the RH and DS6 samples (1.5- and 2.2-fold, respectively, with $p < 0.05$). Thus, in contrast to our results with cleavage by UDG and Ape1, we found no inhibition of pol β activity by the binding of GR-DBD but instead saw a small enhancement.

*DNA Ligase I Activity in Presence or Absence of GR-DBD*—DNA ligase I has been found to be associated with pol β in complexes isolated from bovine testis (24) as well as to perform the ligation function *in vitro* (25–27). In the present study, we examined the activity of DNA ligase I on the dU-containing

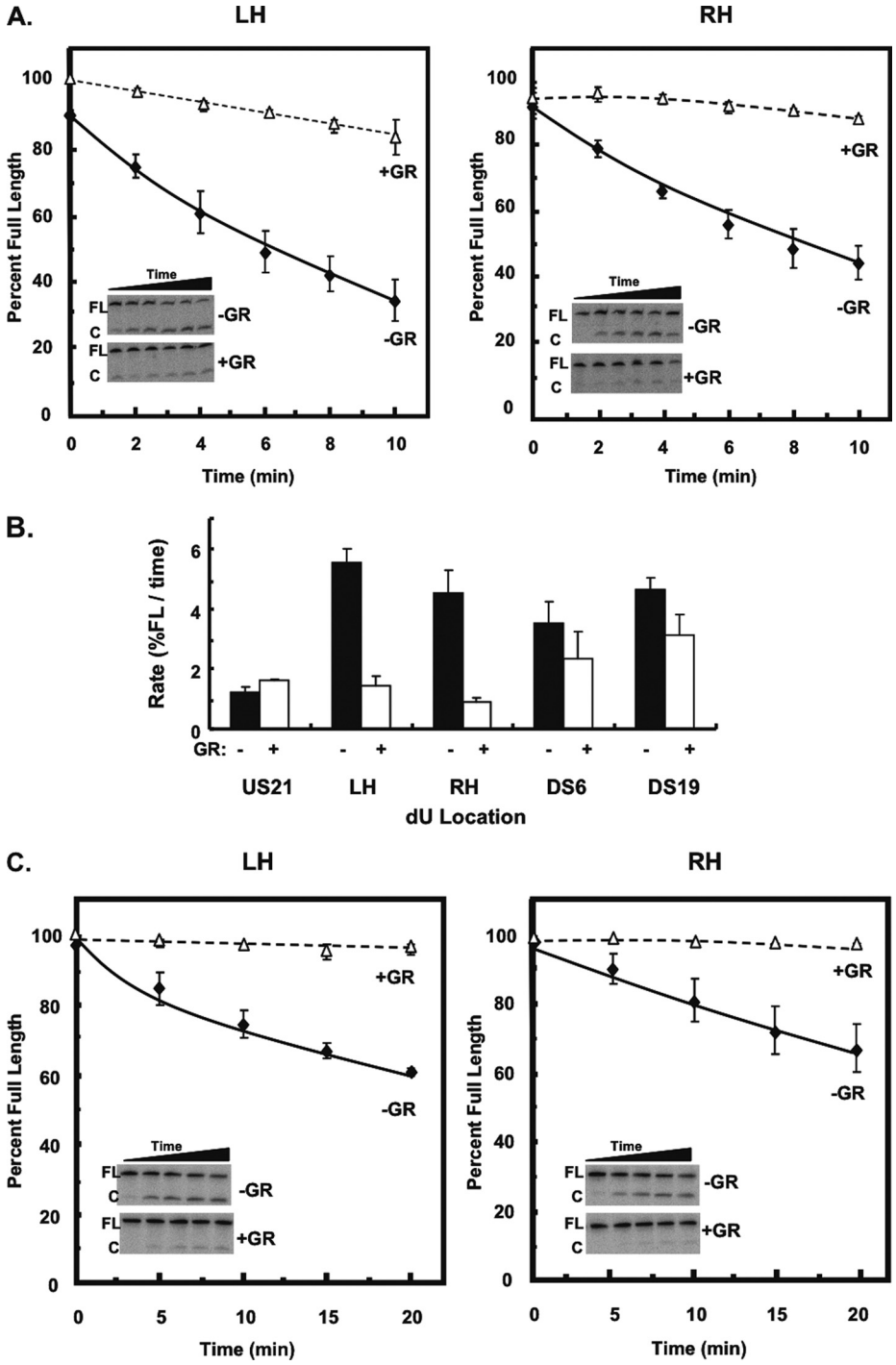


FIGURE 3. **Cleavage of dU-damaged MMTV DNA by UDG and Ape1 with and without bound GR-DBD.** MMTV DNA was labeled at the 5′-end of the top strand and treated with a mixture of UDG (*E. coli*) and Ape1 (human) at 0.025 nM (each) over the course of 10 min. Time points were taken every 2 min. *A*, percentage of full-length DNA *versus* digestion time for U→C substitutions in the LH (*left panel*) or RH (*right panel*) and with (+*GR*; ◇ and *dotted lines*) or without (−*GR*; ◆ and *solid lines*) bound GR-DBD. Values were determined from scans of denaturing polyacrylamide gels showing FL and cleaved (*C*) products over time (*insets*). Each data point represents the mean ± 1 S.D. of at least three independent experiments. *B*, comparison of cleavage rates for the different dU-damaged DNAs. The rates were determined from the initial slopes of the digestion curves (*e.g. A*) as percentage of full length/time. Each *column* represents the mean ± 1 S.D. of the cleavage rates without (*solid bars*) and with (*open bars*) GR-DBD of at least three independent experiments. With the exception of the DS6 samples ($p < 0.07$), all pairs showed significant differences in cleavage rates between +GR-DBD and −GR-DBD samples (US21 and DS19, $p < 0.02$; LH and RH, $p < 0.002$). *C*, MMTV DNA fragments were labeled and treated with a mixture of UDG (human, 0.25 nM) and Ape1 (human, 0.025 nM) as described in *A* with the exception that time points were taken every 5 min for a total of 20 min. Each data point represents the mean ± 1 S.D. of at least three independent experiments for samples without (−*GR*; ◆ and *solid lines*) or with (+*GR*; ◇ and *dotted lines*) GR-DBD bound. (We note that the human enzyme had reduced activity compared with the commercial *E. coli* enzyme and required a 10-fold higher concentration to obtain 40–50% cleavage of FL MMTV fragment within 20 min.)

substrates LH and RH. After treatment by BER enzymes through the pol $\beta$ step, all enzymes were removed from the reaction by PCI extraction, and the nicked fragments were treated with DNA ligase I. Complete repair was measured by the accumulation of full-length product, which did not exceed 65% under the limiting conditions used. As shown in Fig. 5, the activity of DNA ligase I was unaffected by the presence of GR-DBD in either the LH or RH of the GRE.

## DISCUSSION

Upon binding of ligand, the GR translocates into the nucleus where it binds to its cognate sequence, the GRE. Although there is evidence that the receptor can dimerize before it interacts with DNA (28), recognition of the GRE by the GR-DBD has been shown to be cooperative (20), and binding to the low affinity half-site is dependent on the high affinity site being bound (21). The GR-DBD contains five residues that are required for receptor dimerization (22) and behaves similarly to the intact protein, making it ideal for studying GR interactions with DNA. Based on the crystal structure of GR-DBD (15), the damaged nucleotides used in this study do not have specific contacts with the GR-DBD protein. In support of this, we saw no effect of U→C substitution on the ability of GR-DBD to bind to the GRE. Using EMSA and methylation protection assays, we found that GR-DBD bound to dU-damaged DNA with the same affinity as to undamaged DNA.

Based on their crystal structures, both UDG and Ape1 bind one surface (or side) of the DNA molecule (7, 29). However, we found that they were strongly affected by the binding of the GR-DBD on the opposite side of the helix, suggesting that these proteins cannot bind the GRE simultaneously. In the case of UDG, the higher affinity of GR-DBD (5.7 *versus* 48 nM for UDG) (7, 30) must create a steric block to the access of the GRE. In contrast, the binding affinity of Ape1 is significantly

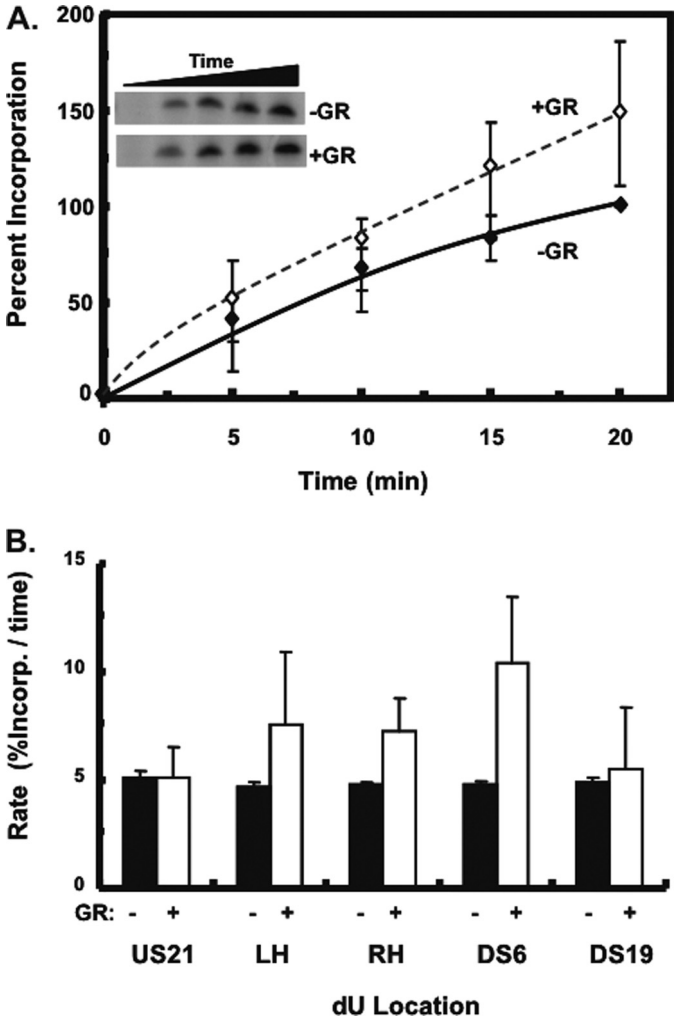


FIGURE 4. **Pol $\beta$ activity on dU-damaged MMTV DNA with and without bound GR-DBD.** *A* and *B*, unlabeled MMTV DNA fragments were initially treated with UDG and Ape1 and then exposed to 1 $\mu$M GR-DBD prior to the addition of 0.05 nM pol $\beta$ and [$\alpha$-$^{32}$P]dCTP. *A*, pol $\beta$ activity on the RH substrate. The panel shows the percentage of incorporation *versus* time without (−*GR*; ♦ and *solid lines*) or with (+*GR*; ◇ and *dotted lines*) bound GR-DBD where values were normalized to the 20-min value for the −GR samples. Values were determined from scans of denaturing polyacrylamide gels showing the accumulation of radiolabeled product over time (*inset*). Each data point represents the mean ± 1 S.D. of at least three independent experiments. *B*, comparison of pol $\beta$ incorporation (*Incorp.*) rates for the different damaged DNAs. Each *column* represents the mean ± 1 S.D. of at least three independent experiments measuring the incorporation rates without (*solid bars*) and with (*open bars*) GR-DBD. Statistically significant differences were seen for samples RH and DS6 ($p < 0.05$).

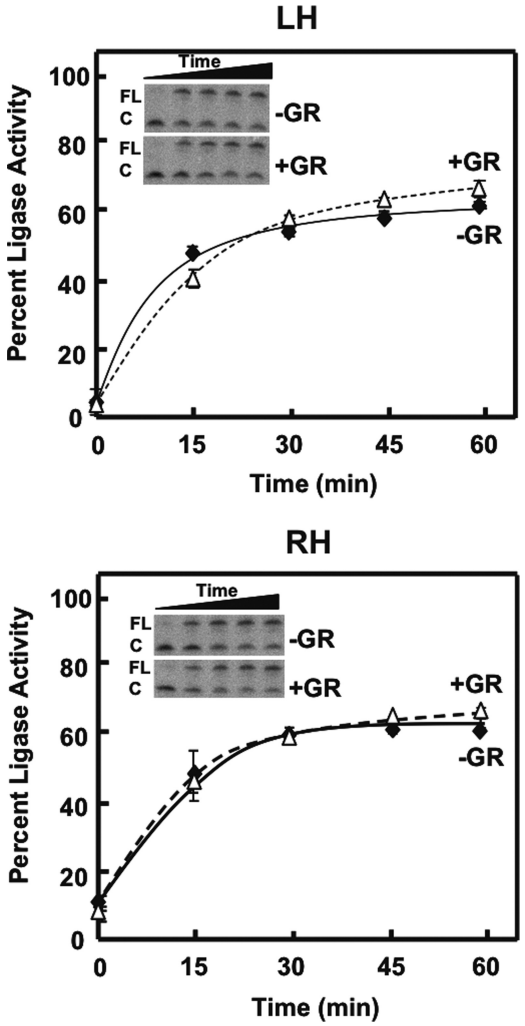


FIGURE 5. **DNA ligase I activity on dU-damaged MMTV DNA with and without bound GR-DBD.** Unlabeled substrate was treated with a 10 nM concentration of both UDG and Ape1 followed by treatment with radiolabeled dCTP and pol $\beta$. Singly labeled substrate was phenol:chloroform-extracted and ethanol-precipitated to remove all enzymes. Substrates (4 pmol) were then treated with 100 nM DNA ligase I over the course of 1 h. Time points were taken every 15 min, and products were run on denaturing polyacrylamide gels. Values were determine from scans of the gels showing FL and cleaved (*C*) products.

higher (0.8 nM $K_d$ (31)), but GR-DBD binding appears to dominate. Thus, competition between GR-DBD and UDG/Ape1 may be the source of slower cleavage.

If competition for GRE binding yields the lag in cleavage activity by UDG/Ape1, there may be a correlation between the affinity of the GR-DBD to each half-site and the amount of interference in the cleavage assay. Indeed, we found that in the presence of saturating levels of GR-DBD a slightly greater reduction in rate was seen for damage to the higher affinity RH (5- or 13-fold) than to the lower affinity LH (3.8- or 10-fold) regardless of the UDG source (*E. coli* or human, respectively). Furthermore, the strongest effect by GR-DBD binding is within the confines of the 15-nucleotide GRE as little difference was seen in cleavage on substrates containing damage just outside this region. The slight decrease seen in DS19 may reflect a change in DNA secondary structure at this site upon GR-DBD binding or nonspecific binding by GR-DBD. (We note that nonspecific binding of GR-DBD is salt-dependent, being partially alleviated at concentrations above 70 mM salt, and the total salt concentration in the GR-DBD binding buffer used was 72.5 mM (32).)

We and others have shown that the activity of pol $\beta$ is suppressed or inhibited when DNA is in a nucleosome (13, 33). The co-crystal structure of pol $\beta$ shows that protein-DNA contacts are extensive, and binding results in an ~90° kink in the DNA (14). Therefore, because DNA wrapped around the histone octamer has reduced torsional flexibility, it is not surprising that pol $\beta$ function is impeded. Here we used naked DNA ± GR-DBD to examine whether a regulatory protein interferes with pol $\beta$ activity similarly to the histone octamer. Indeed,

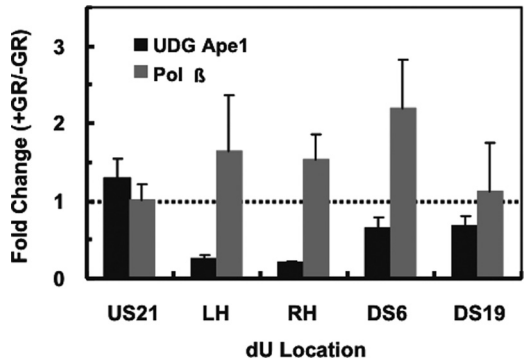


FIGURE 6. **Summary of relative BER enzyme activity (+GR/−GR) at various locations of dU damage in MMTV promoter.** Each *column* represents the mean ± 1 S.D. of the -fold change between +GR and −GR samples for at least three independent experiments. A value of 1 (*dotted line*) denotes no difference in UDG/Ape1 cleavage rates (*solid bars*) or pol β incorporation rates (*gray bars*) when GR-DBD is bound.

based on the reduced rate of cleavage by UDG/Ape1 seen with substrates containing damage in the GRE, we expected a similar trend for pol β. In contrast to our results with nucleosomes, however, we were surprised to see no reduction in pol β activity in the presence of GR-DBD. Furthermore, there was a small enhancement in activity on substrates RH and DS6. If the damaged site is directly "handed to" pol β by Ape1 then this precludes the ability of GR-DBD to physically interfere with this process, and pol β activity would proceed unheeded. As for the slight enhancement, the intrinsic properties of the DNA fragment that are changed by GR-DBD binding (*e.g.* the predicted 35° bend in the helical axis (34)) may enhance pol β activity. Solution structure data of the GR-DBD·GRE complex shows that amino acids 510–517 of the GR-DBD induce DNA bending and unwinding (35), events that might position the abasic site for an easier access by pol β. If so, this could explain the enhancement seen only within the closest proximity to GR-DBD binding.

DNA ligase I has been shown to form a complex with pol β both *in vivo* (24) and *in vitro* (36), forming a multiprotein complex that is responsible for sealing the nick after repair of a damaged nucleotide. This close association presumably results in the priority of DNA ligase I activity over any interference with GR-DBD. After the reduced rate seen at the initial BER steps, it appears that subsequent steps are much less affected by the presence of GR-DBD. Interestingly, the slight enhancement seen for pol β did not correlate with DNA ligase I activity.

Comparison of the results for UDG/Ape1 cleavage and pol β incorporation (Fig. 6) allows one to examine the relationship between the location of damage and the effect on the different enzyme activities. UDG/Ape1 cleavage is greatly reduced within the GRE, whereas in contrast these sites yield unaltered or increased pol β activity. This suggests a complex interplay between the proteins as they compete for access to the substrate. The sequence of events, including the order and duration of protein binding, depends upon the binding affinity of each protein. Initially, we predicted that GR-DBD would physically block access of the repair proteins to the damaged nucleotide. Although this occurred for UDG/Ape1, it was not the case for pol β or DNA ligase I. Importantly, the GR-DBD complex did not create the same block to BER enzymes as the histone octamer. Our results indicate that the ability of BER proteins to access damaged nucleotides is highly dependent on the DNA-protein interactions in place around the damage site. Clearly, it will be of interest to compare the repair efficiency and mutation rates within different locations of chromatin of intact cells and under different regulatory conditions.

*Acknowledgments—We thank Drs. Samuel H. Wilson and Rajendra Prasad (Laboratory of Structural Biology, NIEHS, National Institutes of Health) for providing recombinant pol β and DNA ligase I; Dr. Keith Yamamoto (Department of Cellular and Molecular Pharmacology, University of California, San Francisco) for providing pGR440 GR-DBD expression plasmid; and Drs. William B. Davis, John M. Hinz, and Anamaria Zavala (School of Molecular Biosciences, Washington State University) for helpful discussions and critical evaluation of this manuscript.*

## REFERENCES

1. Friedberg, E. C., Walker, G. C., Siede, W., Wood, R. D., Schultz, R. A., and Ellenberger, T. (2006) *DNA Repair and Mutagenesis*, 2nd Ed., American Society for Microbiology Press, Washington, DC
2. Hanawalt, P. C. (2007) *Mol. Cell* **28,** 702–707
3. Conconi, A., Liu, X., Koriazova, L., Ackerman, E. J., and Smerdon, M. J. (1999) *EMBO J.* **18,** 1387–1396
4. Kwon, Y., and Smerdon, M. J. (2003) *J. Biol. Chem.* **278,** 45451–45459
5. Kwon, Y., and Smerdon, M. J. (2005) *Mutat. Res.* **577,** 118–130
6. Huffman, J. L., Sundheim, O., and Tainer, J. A. (2005) *Mutat. Res.* **577,** 55–76
7. Parikh, S. S., Mol, C. D., Slupphaug, G., Bharati, S., Krokan, H. E., and Tainer, J. A. (1998) *EMBO J.* **17,** 5214–5226
8. Wilson, S. H., and Kunkel, T. A. (2000) *Nat. Struct. Biol.* **7,** 176–178
9. Dianov, G. L., and Parsons, J. L. (2007) *DNA Repair* **6,** 454–460
10. Memisoglu, A., and Samson, L. (2000) *Mutat. Res.* **451,** 39–51
11. Ghosh, R., and Mitchell, D. L. (1999) *Nucleic Acids Res.* **27,** 3213–3218
12. Verri, A., Mazzarello, P., Biamonti, G., Spadari, S., and Focher, F. (1990) *Nucleic Acids Res.* **18,** 5775–5780
13. Beard, B. C., Wilson, S. H., and Smerdon, M. J. (2003) *Proc. Natl. Acad. Sci. U.S.A.* **100,** 7465–7470
14. Sawaya, M. R., Prasad, R., Wilson, S. H., Kraut, J., and Pelletier, H. (1997) *Biochemistry* **36,** 11205–11215
15. Luisi, B. F., Xu, W. X., Otwinowski, Z., Freedman, L. P., Yamamoto, K. R., and Sigler, P. B. (1991) *Nature* **352,** 497–505
16. Clemens, K. R., Zhang, P., Liao, X., McBryant, S. J., Wright, P. E., and Gottesfeld, J. M. (1994) *J. Mol. Biol.* **244,** 23–35
17. Payvar, F., DeFranco, D., Firestone, G. L., Edgar, B., Wrange, O., Okret, S., Gustafsson, J. A., and Yamamoto, K. R. (1983) *Cell.* **35,** 381–392
18. Scheidereit, C., Geisse, S., Westphal, H. M., and Beato, M. (1983) *Nature* **304,** 749–752
19. Ham, J., Thomson, A., Needham, M., Webb, P., and Parker, M. (1988) *Nucleic Acids Res.* **16,** 5263–5276
20. Tsai, S. Y., Carlstedt-Duke, J., Weigel, N. L., Dahlman, K., Gustafsson, J. A., Tsai, M. J., and O'Malley, B. W. (1988) *Cell* **55,** 361–369
21. Dahlman-Wright, K., Siltala-Roos, H., Carlstedt-Duke, J., and Gustafsson, J. A. (1990) *J. Biol. Chem.* **265,** 14030–14035
22. Dahlman-Wright, K., Wright, A., Gustafsson, J. A., and Carlstedt-Duke, J. (1991) *J. Biol. Chem.* **266,** 3107–3112
23. Buetti, E., and Kühnel, B. (1986) *J. Mol. Biol.* **190,** 379–389
24. Prasad, R., Singhal, R. K., Srivastava, D. K., Molina, J. T., Tomkinson, A. E., and Wilson, S. H. (1996) *J. Biol. Chem.* **271,** 16000–16007
25. Srivastava, D. K., Berg, B. J., Prasad, R., Molina, J. T., Beard, W. A., Tomkinson, A. E., and Wilson, S. H. (1998) *J. Biol. Chem.* **273,** 21203–21209
26. Kubota, Y., Nash, R. A., Klungland, A., Schär, P., Barnes, D. E., and Lindahl, T. (1996) *EMBO J.* **15,** 6662–6670
27. Nicholl, I. D., Nealon, K., and Kenny, M. K. (1997) *Biochemistry* **36,** 7557–7566

28. Cairns, W., Cairns, C., Pongratz, I., Poellinger, L., and Okret, S. (1991) *J. Biol. Chem.* **266,** 11221–11226
29. Mol, C. D., Hosfield, D. J., and Tainer, J. A. (2000) *Mutat. Res.* **460,** 211–229
30. Dahlman-Wright, K., Wright, A., Carlstedt-Duke, J., and Gustafsson, J. A. (1992) *J. Steroid Biochem. Mol. Biol.* **41,** 249–272
31. Strauss, P. R., Beard, W. A., Patterson, T. A., and Wilson, S. H. (1997) *J. Biol. Chem.* **272,** 1302–1307
32. Härd, T., Dahlman, K., Carlstedt-Duke, J., Gustafsson, J. A., and Rigler, R. (1990) *Biochemistry* **29,** 5358–5364
33. Nilsen, H., Lindahl, T., and Verreault, A. (2002) *EMBO J.* **21,** 5943–5952
34. Bishop, T. C., and Schulten, K. (1996) *Proteins* **24,** 115–133
35. Harris, L. F., Sullivan, M. R., Popken-Harris, P. D., and Hickok, D. F. (1994) *J. Biomol. Struct. Dyn.* **12,** 249–270
36. Dimitriadis, E. K., Prasad, R., Vaske, M. K., Chen, L., Tomkinson, A. E., Lewis, M. S., and Wilson, S. H. (1998) *J. Biol. Chem.* **273,** 20540–20550